文章编号:1000-8055(2019)01-0034-11 doi:10.13224/j.cnki.jasp.2019.01.005

Design and application of an air-cooled probe for total pressure measurement at combustor outlet

LIU Xupeng, SUN Qi, WANG Xiaoliang, XUE Xiusheng, YIN Dong

(Shenyang Engine Research Institute,
Aero Engine Corporation of China, Shenyang 110015, China)

Abstract: An air-cooled probe was designed for measurement of total pressure at combustor outlet; its cooling scheme combined the film cooling and convection cooling. With the aid of CFD technique, cooling effectiveness of the coolant jets at various blow ratios was compared; suitable blow ratios and configuration of film holes were chosen accordingly. The overall cooling performance of the probe was evaluated via CFD technique, the design was improved according to the simulation result, and the cooling effect of the leading edge was obviously strengthened by increasing the local coolant mass flow rate. The results of wind tunnel test indicated that, between Mach numbers 0.2 and 0.4, the probe achieved a high accuracy at various attack angles. The probe was utilized in an annular combustor rig test, the highest temperature reached 1 760 K and total pressure reaches 1036 kPa. The result of rig test demonstrates that the coolant film distribution consistent appropriately with the CFD results.

Key words: high temperature measurement; total pressure; probe; film cooling; CFD; combustor outlet

CLC number: V221.72 **Document code**: A

Annular combustor rig test aims to evaluate the combustion stability, combustion efficiency, cooling effect, temperature profile of outlet and pressure loss etc. of the combustor. The pressure recovery factor acquired in annular combustor test is a key parameter of combustor performance, which can be used to predict the efficiency of the engine and the performance of cooling system. Currently, the most direct and effective approach to measure the combustor outlet pressure profile is the utilization of immersion probe. However, the pressure and temperature of the gas of combustor outlet are both extremely high reaching 3.5 MPa and 1800 K respectively; the highest temperature can go beyond 2000 K, which far exceeds the melting temperature of nickel-based alloys. For this extreme circumstance, two schemes are considered in the design of immersion probe of combustor outlet:

1) To apply high temperature resistance materials.

2) To implement cooling configuration onto the probe.

According to the state of the art, the material can be used in this extreme circumstance is the ceramic material. In Ref.[1], Yang Can et al. designed a small size thermocouple probe employing ceramic material as structural components; its calibration temperature reaches 1960.6 K, whereas it is only used as a reference in calibration, not in a real combustor test[2]. Liu Liping et al.[3] utilized ceramic material in a water-cooled probe as a shielding casing of the thermocouple which works as a non-structural component. In summary, because of its poor thermal fatigue property, the ceramic material cannot be widely used as structural components.

Another design scheme is cooling configura-

Received: 2017-12-21

Citation: LIU Xupeng, SUN Qi, WANG Xiaoliang, et al. Design and application of an air-cooled probe for total pressure measurement at combustor outlet[J]. Journal of Aerospace Power, 2019, 34(1): 34-44.

tion. Its mechanism is that by introducing coolant, mainly water and air, the support of the immersion probe is cooled down below its melting point in hot gas. Plana et al. designed a water cooled sample probe for gas analysis; in the design, the cooling water is discharged out of the test rig after a circulation in the probe, in this process heat transfer is accomplished. To avoid excessive load to the probe, the pressure of the water varies following the pressure variation of the flow in combustor chamber simultaneously[4]. Wang Mingrui et al. designed a water cooled probe which discharges water into the flow field of combustor outlet directly after it has cooled down the probe[5]. The merit of water cooled configuration is the excellent cooling effect; however, there is significant drawback that to avoid extremely local high stress inside the probe at low pressure conditions, the pressure of cooling water should be adjusted simultaneously with the pressure of gas flow in combustor chamber, this increases the complexity of cooling system significantly. In addition, in subsonic flow, disturbances in the flow field will influence the upstream flow filed in certain extent[6], thus water discharged into the flow field might deteriorate the performance of combustor. Yang Can et al. designed a film cooled thermocouple probe employing air as coolant[2]. Although the thermal conductivity of air is much lower, air cooled probe's cooling performance can be improved by introducing advanced cooling technique; it also has the advantage like sharing the same high pressure air source with the combustor, so that the pressure of coolant can vary simultaneously with the gas flow in combustor chamber.

The principle of film cooling is by introducing secondary flow onto the surfaces exposed in the hot gas from discrete holes to protect the local and downstream regions[7]. The dimensions of the film hole are one of the key factors influencing the cooling effectiveness of film cooling[8]. Haven et al. used PIV technique to investigate the main reason causing cooling film detachment; it is found that the kidney-shaped vortices caused by the boundary layer of the holes lifts the film off the surface in many cases. Thus, a good design can delay the formation of kidney-shaped vortices to make film attach to the surface properly[9]. In the past 4 decades, researchers have done a lot of work to study how the cooling performance is influenced by the dimensions of film holes[10]. Han et al. studied the cooling effectiveness of various shapes of film hole in experiments; the results indicate that when blow ratio varies between 0.6 and 1.2, the diffuser shaped (fan shaped) holes has better cooling effectiveness than cylindrical holes, even in unsteady conditions[11]. Hyams et al. compared five distinct configurations of film hole via CFD technique, the investigation showed that, at chosen blow ratios, the laterally diffused film holes have the best coverage and cooling effectiveness[12]. Chen et al. compared the performances of backward and forward injections in experiments. It is found that due to the lateral spread and mixing effects, when blow ratio is 2.0, the performance of backward injection is better, however its drawbacks are obvious that it disturbs the upstream flow leading to significant pressure loss and increases local convection heat transfer coefficient remarkably[13].

Another factor influences film cooling effect significantly is density of coolant. Liu et al. investigated how the coolant density influences the cooling effect of high pressure turbine guide vane via PSP technique. The result shows when the density ratio of coolant to hot gas increases, the cooling effectiveness on the suction side of the blade increases proportionally; especially when density ratio increases from 1.0 to 1.5, the effectiveness increases substantially[14]. Diganta et al. studied the film cooling effectiveness of a turbine rotor blade; it is found that when coolant density increases, the cooling effectiveness of pressure side increases proportionally; while on the suction side between 45% and 75% chord length, the cooling effectiveness increase dramatically[15].

In the present paper, a film cooled probe employing air as coolant is designed and applied for an annular combustor rig test.

1 Demands of the design

1.1 Main parameters of the combustor testing

The demand to the probe are from a testing project of an annular combustor of a turbofan engine, the parameters of the most severe experiment condition are shown in Table 1.

Table 1 The parameters of the highest testing point of an annular combustor

Parameters	Value
Inlet pressure/kPa	1500
Inlet temperature/K	863
Inlet mass flow rate/(kg/s)	32.55
Average outlet temperature/K	1800

1.2 Aims of the design

The aims of the design can be summarized as:

1) When the flow attack angle varies between $-5°$ and $+5°$, the accuracy of measurement should be at least 0.3%.

2) In 1800 K gas, the outer surface temperature of the probe should be below 1223 K (the endurable temperature of nickel-based alloys).

3) Seven sensing heads should be placed radially along the leading edge of the probe to sense the stagnation pressure.

4) The blockagerate caused by four probes all together should be less than 3% of the area of the flow path.

1.3 Working principle of the probe

The working principle of the probes is shown in Fig. 1. The probe (Fig. 2) is fixed on a traverse gear at outlet of the combustor. When the combustor is being tested, the probe rotates with the traverse gear to scan the flow field of the combustor outlet. The cooling air is transmitted into the probe from the internal ventilation chamber of the traverse gear, and then discharged out of the discrete film holes and forming a thin layer of protection film on the outer surface of the probe. The traverse gear and the casing of the flow path are both cooled by water. Stagnation pressure is measured via the sensing heads on the leading edge of the probe and then transmitted to the data acquisition system.

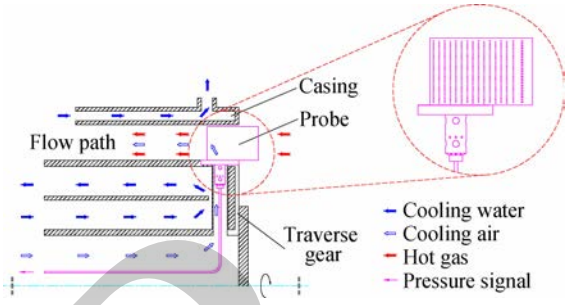

Fig. 1 The working principle of the probe

Fig. 2 The air-cooled total pressure probe

2 Sensing head design

There are mainly three kinds of sensing-heads for total pressure measurement[16], which are demonstrated in Fig. 3. The features of these sensing heads are listed below:

1) The L-shaped sensing head reduces the inference from the support significantly, can achieve a quit high accuracy to a wide range of attack angles; its insensitivity to attack angle variation achieves approximately $\pm 15°$.

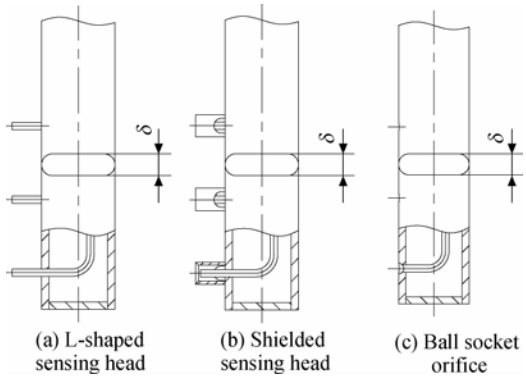

Fig. 3 Configuration of three main sensing heads

2) The shielded sensing head adds a cylindrical shield around the L-shaped head, to adjust the inlet flow to increase the insensitivity of probe,its maximum insensitivity achieves about ±45°.

3) The ball socket orifice sensing head is located on the leading edge of the support, because there is nothing extends out of the support, the size of the probe could be compact and the mechanical integrity of the probe is the best of all, its insensitivity is approximately ±15°.

The L-shaped and the shielded sensing head have higher accuracy and wider insensitivity range,they are often used in the situations that the flow attack angles vary markedly. In consideration of the severe condition mentioned above, the components extending out of the support are quite difficult to be cooled. In addition, the flow attack angle does not vary significantly at the outlet of combustor. Therefore, the ball socket orifice is chosen due to its good mechanical integrity and cooling performance.

3　Design of film hole

3.1　Methodology and main design parameters

There are two main parameters should be considered in the design of the film holes: the configuration of film holes and the properties of coolant. The procedure of design is shown in Fig. 4. The dimension of a single film hole is determined in the first place; then the film cooling effectiveness is evaluated via CFD technique; at last, the distance between film holes is determined according to CFD simulation results.

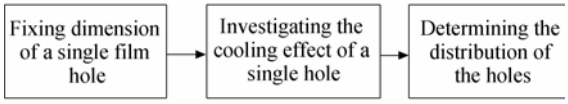

Fig. 4　Design procedure of film holes

The effectiveness of film cooling can be expressed as:

$$\eta_t = \frac{T_g - T_{aw}}{T_g - T_c} \tag{1}$$

Where, η_t represents film cooling effectiveness; T_g and T_c represent temperature of gas and cooling air respectively; T_{aw} is adiabatic wall temperature which equals to the recovery temperature of hot gas in vicinity of the surface.

To insure the probe works in the hot gas reliably, the wall temperature should be less than the allowable working temperature of the material (normally 1223 K for nickel-based alloys)[17]. Therefore, the value of T_{aw} is 1223 K, substituting T_{aw} and other known parameters into Eq. (1), the film cooling effectiveness can be calculated as:

$$\eta_t = 0.4$$

It has been proved by experiments that film cooling effectiveness is determined by two non-dimensional parameters[18], see Eq. (2). Based on different conditions, researchers acquired various expressions of film cooling effectiveness; however, there is not a general equation could handle all the situations. Therefore, in this design, according to the working condition of the annular combustor, CFD technique is introduced to evaluate the cooling effectiveness.

$$\eta = f(M, X) \tag{2}$$

In Eq. (2) M represents blow ratio of cold to hot gas, it is expressed in Eq. (3).

$$M = \frac{\rho_c v_c}{\rho_g v_g} \tag{3}$$

Where, ρ_c and ρ_g are densities of cold and hot gas, respectively; v_c and v_g are velocities of cold and hot gas, respectively.

In Eq. (2) X represents the non-dimensional distance downstream the film hole, its expression is in Eq. (4)

$$X = \frac{x}{d} \tag{4}$$

Where x represents the distance downstream the film hole, d represents the diameter of film hole.

Limited by the testing rig, the main parameters of the cooling air have already been restricted at the maximum test point; the range of pressure of the cooling air is from 1.42 MPa to 1.5 MPa and its temperature is about 310 K. Since the parameters of the hot gas at combustor

outlet has been known, consequently the range of blow ratio is determined as:

$$0.5 \leqslant M \leqslant 2.0$$

3.2 CFD simulation

Although it has been mentioned in Refs. [11] and [12] that the fan-shaped film holes have better cooling performance, cylindrical film holes also have acceptable cooling performance and are easier to manufacture, so the cylindrical film holes with diameter of 0.5 mm are chosen in the design. Theoretically, the smaller the angle between film holes and probe surface, the better coverage performance can be acquired, unfortunately the angle is restricted by practical manufacture capability, so 30° is chosen in the design. To sum up, the dimension of a single film hole is shown in Fig. 5 where 1.5 mm is the thickness of the probe wall.

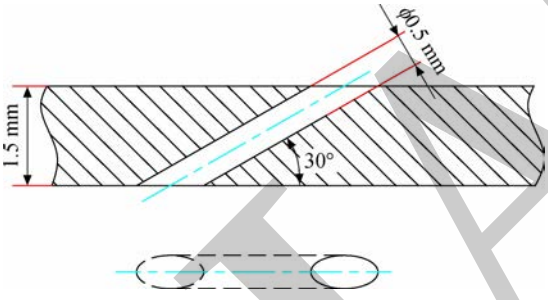

Fig. 5 Dimension of a single film hole

To evaluate the cooling performance of a single film hole at various blowratios and choose an appropriate distance between film holes, the cooling effectiveness of a single film hole should be evaluated firstly via CFD. The simulation was operated in the commercial code CFX. The model utilized in the simulation is shown in Fig. 6, the number of the grid is about 230 000, the turbulence equation is k-ε, high resolution scheme is chosen. The boundary conditions of hot gas are chosen from Table 1. The temperature of coolant is 310 K and pressure varies from 1.42 MPa to 1.5 MPa, which are limited by the testing rig.

Figure 7 demonstrates the cooling effectiveness contours of a single film hole at different blow ratios. It can be seen that when $M=0.5$

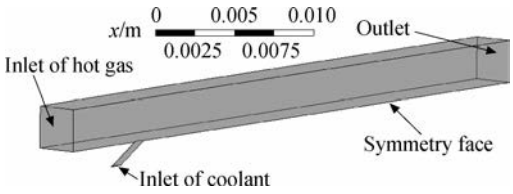

Fig. 6 The physical model used in CFD simulation

and $M=1.0$, the coolant covers the downstream surface appropriately; while when $M=1.5$ and $M=2.0$, the area covered by the coolant is much smaller. The reason of this phenomenon is that when blow ratio increases, the momentum of the coolant jet increases accordingly, so the kidney-shaped vortices caused by the boundary layer of film hole are enhanced significantly, which lifts the coolant film off the surface. In Fig. 7(b), Fig. 7(c) and Fig. 7(d), the two branches appear at the rear of the jet proves the existence of the kidney-shaped vortices, due to the hot gas involved into the coolant jet by counter rotation of the kidney-shaped vortices, the cooling effectiveness along the central line is lower than the edges of the jet.

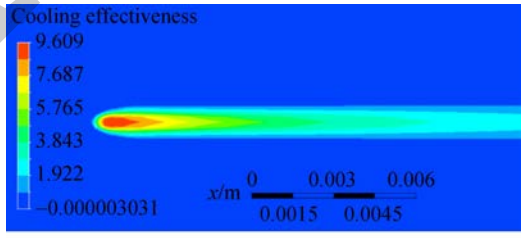

(a) M=0.5

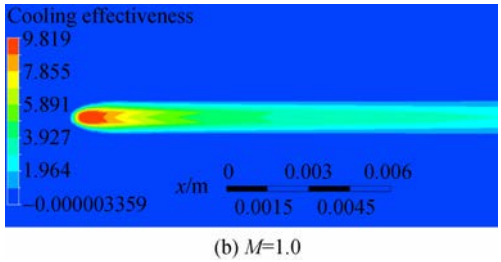

(b) M=1.0

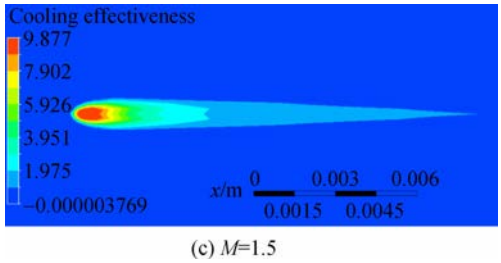

(c) M=1.5

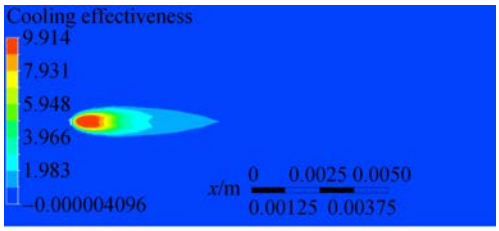

(d) M=2.0

Fig. 7　Cooling effectiveness contour of a single film hole

Figure 8 shows the contours of cooling effectiveness of jets at various blow ratios. It can be seen that when $M=0.5$ and $M=1.0$, the jet attaches to the surface appropriately; while when $M=1.5$ and $M=2.0$, the jet detaches the surface after a certain distance, this verifies the trends shown in Fig. 7(c) and Fig. 7(d). Compare Fig. 8(a) and Fig. 8(b), when $M=0.5$, due to smaller momentum of the jet, it attaches to the surface tightly when just leaving the hole. However, when the jet goes downstream, because of the effect of dilution and mixing, its cooling effectiveness decreases obviously. When $M=1.0$, although a trend of detachment can be seen when the jet just leaves the hole, because of larger mass flow rate of the coolant, its capability to resist dilution and mixing effect is strengthened, therefore its cooling effectiveness does not see steep drop when the jet flows downstream.

Figure 9 illustrates the curves of film cooling effectiveness of a single film hole at various

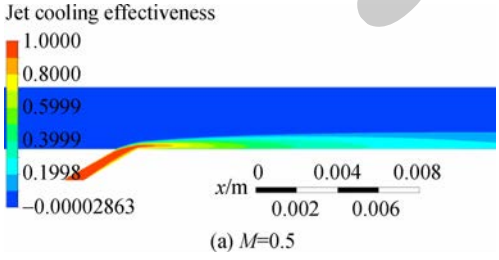

(a) M=0.5

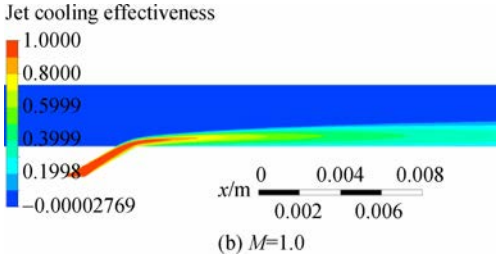

(b) M=1.0

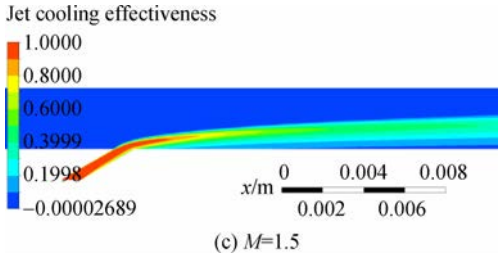

(c) M=1.5

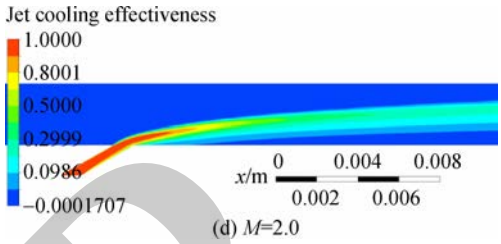

(d) M=2.0

Fig. 8　Cooling effectiveness contour of the coolant jet

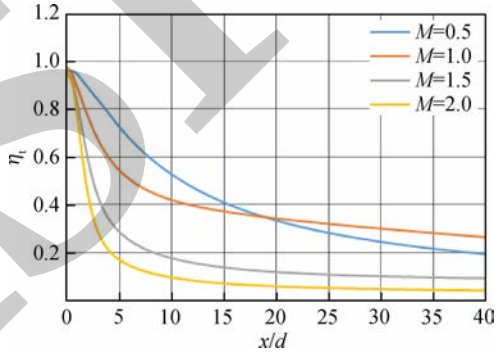

Fig. 9　CFD results of cooling effectiveness downstream the film cooling hole

blow ratios. When blow ratio is between 0.5 and 2.0, it can be seen that in the process of coolant jet flowing downstream, the cooling effectiveness of the jet reduces due to the effect of dilution and mixing. When the jet just leaves the hole, the film cooling effectiveness sees a steep drop. Whereas, when x/d keeps increasing, the falling of cooling effectiveness becomes much smoother. Notably, when x/d is higher than 18, the cooling effectiveness of $M=1.0$ overtakes $M=0.5$, this phenomenon verifies the analysis above that higher blow ratio indicates higher capability to resist dilution and mixing.

In brief, when blow ratio is between 0.5 and 1.0, the film cooling effectiveness achieves relatively satisfying results. Thus, to guarantee the blow ratio to be limited in this range, the

pressure of coolant should be maintained between 1.42 MPa and 1.435 MPa.

To minimize the burden of cooling system and increase the robust performance of the probe, according to Fig. 9, the value of x/d is chosen to be 12, to guarantee when blow ratio varies between 0.5 and 1.0, the value of film cooling effectiveness is above 0.4.

4 Investigation and improvement of overall cooling performance

To measure the total pressure of the hot gas precisely, the film holes are not allowed to be placed on the leading edge of the probe to avoid disturbance to the main flow. Thus, there is only one option left for leading edge cooling, the internal convection cooling. Whereas due to direct impingement of hot gas, generally the temperature of the leading edge is the highest of the probe. In addition, because the flow field of coolant inside the probe is not uniform, the cooling effect of the probe is not uniform, too. Hence, the overall cooling effect of the probe must be evaluated to predict the local cooling performance on the probe. According to the overall cooling performance of the probe, improvements can be implemented accordingly.

CFD technique is introduced to analyze heat transfer and aerodynamic performance of the probe, to simplify the simulation process some assumptions are introduced in the first place:

1) The heat conduction between probe and water cooled casing of flow path is ignored.

2) The radiation heat transfer between probe and water cooled casing of flow path is ignored.

3) The average blow ratio is 1.0, which is the worst condition of the design.

4) The temperature profile of the combustor outlet is uniform.

4.1 The original design

To simplify the simulation, according to Eq. (5), the discrete film holes can be converted to equivalent slots[18].

$$S_e = \frac{\pi d^2}{4t} \tag{5}$$

Where S_e represents equivalent width of the slot, d represents diameter of the film hole, t represents equivalent length of the slot.

The simplified 3-D model of the probe and the fluid domain are shown in Fig. 10. The simulation is also carried out in CFX code, the number of grid is approximately 1.2 million, the turbulence equation is k-ε, high resolution scheme is chosen. The input parameters of combustor outlet are chosen from Table 1 and the parameters of the coolant are pressure 1.435 MPa and temperature 310 K which imply the worst cooling effectiveness of the design.

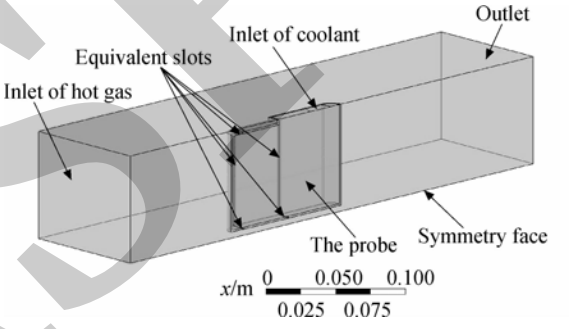

Fig. 10 3-D model of the simplified probe and fluid domain

The temperature contour is shown in Fig. 11. It can be seen that due to the mutual effect of film cooling and internal convection cooling the probe is properly cooled, the average temperature of the probe is 617.7 K and the highest temperature 1 088 K appears on the leading edge because of the absence of film cooling and the direct impingement of hot gas.

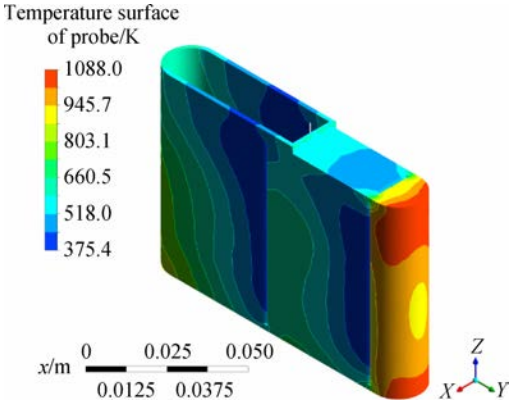

Fig. 11 Temperature contour of the original design

The internal coolant streamlines are shown in Fig. 12, a large low-speed back-flow region can be seen at trailing edge of the probe, according to heat transfer theory the local convection heat transfer rate will be quite low[19]. However, with the protection of upstream film, the local temperature remains in an acceptable range (see the temperature contour of trailing edge in Fig. 11). Notably, at the two corners of internal leading edge, there are two low-speed regions which make the local convection heat transfer rate reduces significantly; furthermore, the absence of film cooling makes the situation more severe, therefore the highest temperature of the probe appears here (see the temperature contour of leading edge in Fig. 11).

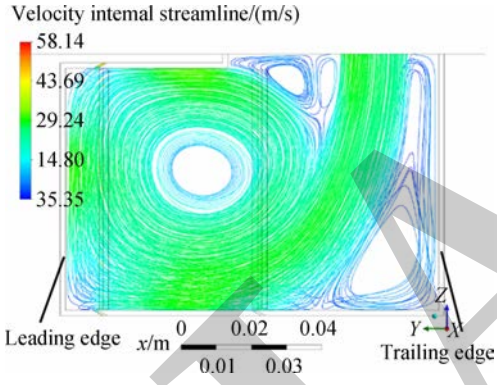

Fig. 12　Streamlines of internal probe

4.2　The improved design

To enhance internal convection heat transfer of the leading edge, in the improved design the areas of the film holes next to the leading edge are increased with other dimensions remaining the same. The purpose of the improvement is increasing the coolant mass flow rate of leading edge to enhance local convection heat transfer while the coolant mass flow rate of the other parts remains the same. The comparison of the dimension of the equivalent slots next to the leading edge of original design and improved design is shown in Fig. 13. The width of the equivalent slot next to the leading edge of the improved design is 1.25 times of the original design.

The same model and boundary conditions

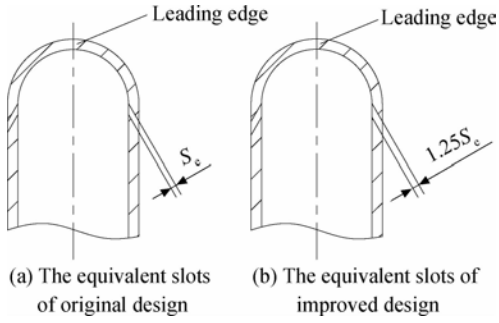

Fig. 13　Comparison of the equivalent slots next to the leading edge between original and improved design

settings with the original design are set in the simulation. The simulation results show that the coolant mass flow rate of the probe is increased from 60 g/s in the original design to 65 g/s in the improved design. The outer surface temperature contour of the improved probe is demonstrated in Fig. 14. It can be seen that although the trend of temperature distribution does not vary substantially, the highest temperature of improved design reduces 29 K from 1 088 K in the original design to 1 059 K. Due to the increase of coolant mass flow rate, the area of low temperature regions of front part extends significantly; the average temperature of the improved design reduces from 617.7 K in the original design to 603.4 K.

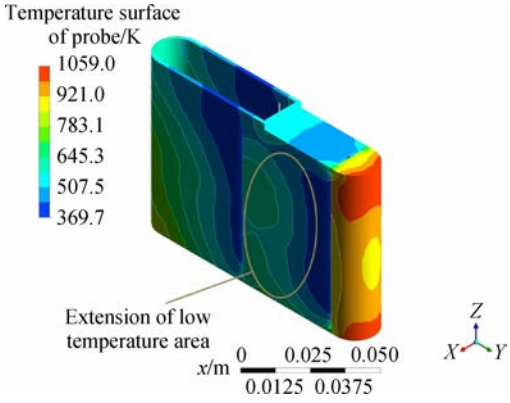

Fig. 14　Temperature contour of the improved design

Fig. 15 indicates the radial temperature distribution of the probe leading edge, the horizontal axil represents the relative height of the leading edge and the vertical axil represents the temperature of the outer surface. It can be seen that

because of the increase of coolant mass flow rate, the overall temperature of the leading edge sees an obviously reduction. The average temperature reduces from 1 001 K to 969.9 K. The temperature profile along the middle span of the probe is demonstrated in Fig. 16, the horizontal axial represents relative distance to the leading edge and the vertical axial represents the temperature of the surface. It is shown that temperature of the outer surface between the leading edge and the first slot sees an obvious drop; temperature between two slots sees a drop in certain extent. Because no modification is implemented to the second slot, no obvious change can be seen at the rear region of the probe.

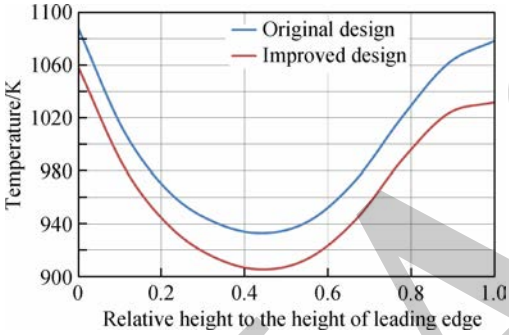

Fig. 15 Temperature profile along the leading edge of the probe radially

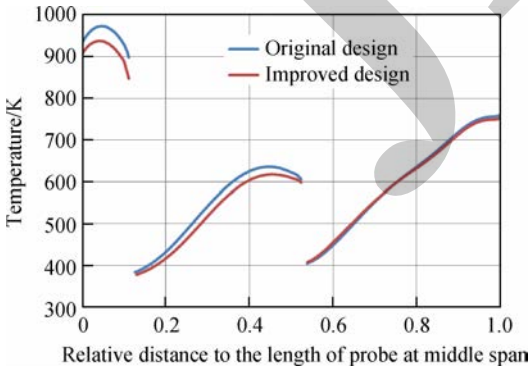

Fig. 16 Temperature profile along the middle span of the probe

4.3 The results of wind tunnel calibration test

To investigate the accuracy of the probe at various Mach numbers, a wind tunnel test has been implemented. The probe being calibrated in wind tunnel in shown in Fig. 17. According to the conditions of flow field at the combustor outlet, the Mach number is relatively low and the attack angle of the flow does not vary significantly; hence the calibration points are chosen as: attack angle between $-15°$ and $+15°$ and Mach number between 0.2 and 0.4 with step 0.1. The calibration curves are shown in Fig. 18.

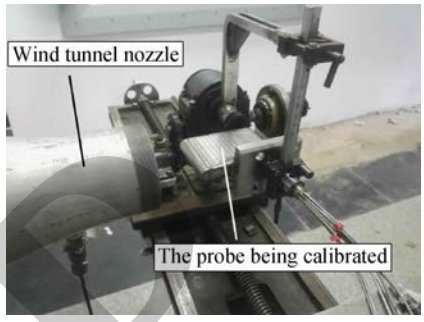

Fig. 17 The probe being calibrated in wind tunnel

It can be seen in Fig. 18, at $Ma=0.2$ the error is lower than 0.3% when the attack angle range is between $\pm10°$. The definition of the error of the probe is expressed in Eq. (6). At $Ma=0.3$ and $Ma=0.4$ the error is below 0.3% when the attack angle range is between $\pm5°$.

$$E=\frac{p-p_{\text{measured}}}{p} \tag{6}$$

Where E represents the error of the meas-

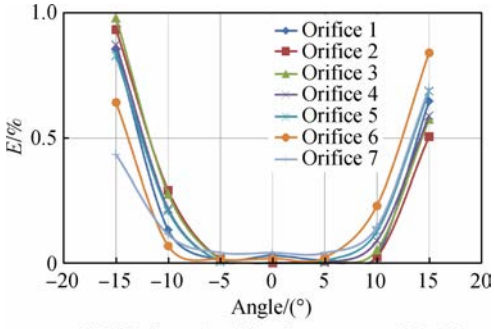

(a) Wind tunnel calibration curves at Ma=0.2

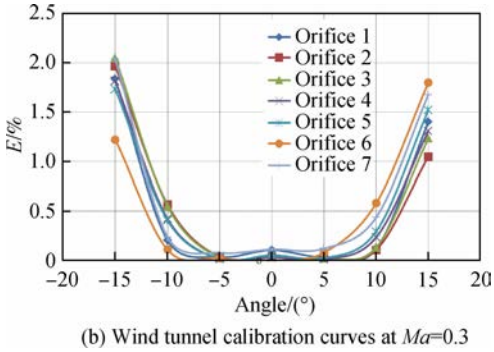

(b) Wind tunnel calibration curves at Ma=0.3

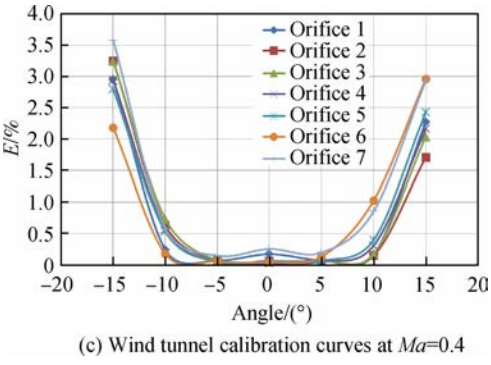

Fig. 18　Calibration curves from wind tunnel test at various Mach numbers

urement, p represents total pressure of the wind tunnel, $p_{measured}$ represents the total pressure measured via the probe.

5　Application in experiment

The probe was used in the annular combustor tests for 6 times, the maximum working condition has achieved total pressure 1036 kPa, temperature 1 760 K. The details of working conditions are listed in Table 2.

Table 2　Working conditions of the probe

Test No.	Average total pressure of combustor outlet/kPa	Maximum temperature of combustor outlet/K
1	450	1081
2	475	1569
3	475	1559
4	994	1499
5	477	1760
6	1036	1760

The probe used in the experiments is shown in Fig. 19, it can be seen that because of the directly impingement of hot gas and the absence of the protection of coolant film, the leading edge sees obvious black trace, which indicates it has been severely burnt. The regions marked by the red dash lines sees clear traces burnt by hot gas; compared with the pressure contour of coolant inside the probe in Fig. 20, these burnt regions consists properly with the high pressure region. Due to the high pressure of coolant, the blow ratio in these regions raises and the coolant film tends to detach the surface, consequently hot gas invades into the gaps between the adjacent film holes. On the contrary, the region enclosed by blue solid line maintains the original appearance of the metal; it indicates that in the region the coolant film attaches onto the surface appropriately due to the relatively low pressure and a modest blow ratio, this is also appropriately consistent with the low pressure region in Fig. 20. As a result, it is evident that the result of the experiment consists properly with the CFD simulation.

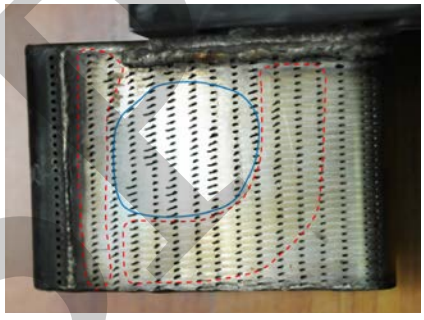

Fig. 19　The probe used in experiments

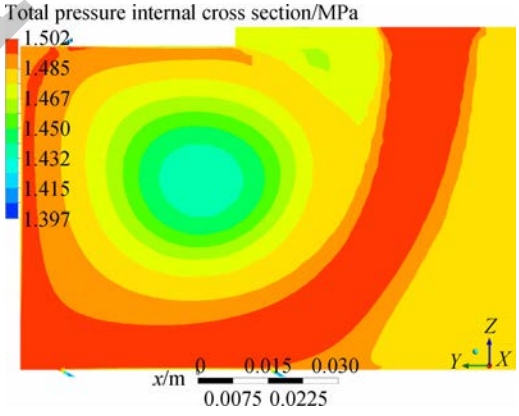

Fig. 20　Pressure contour of coolant inside the probe

6　Conclusion

An air cooled probe for total pressure measurement of hot gas at combustor outlet is designed. With the assistance of CFD technique, the configuration of film holes on the probe is designed. The overall cooling effect of the probe is evaluated and then improved according to the simulation results. The accuracy of the probe is investigated in wind tunnel. The probe is eventually

utilized in an annular combustor rig test successfully. The conclusions are summarized below:

a) According to the results of CFD simulation, to obtain a satisfying cooling effect, the blow ratio should be between 0.5 and 1.0. The non-dimensional distance between two film holes should be at least 12 for a good cooling performance.

b) According to the result of CFD simulation, at maximum working condition, average temperature of the probe of original design is 617.7 K, the maximum temperature locating at the leading edge is 1088 K.

c) By increasing local coolant mass flow rate of the leading edge, at the highest working condition, the average temperature of the probe reduces to 603.4 K; the highest temperature reduces to 1059 K in the improved design.

d) According to the results of wind tunnel experiment, for accuracy of 0.3%, the insensitivity range of the probe is between ±10° at $Ma=0.2$ and between ±5° at $Ma=0.3$ and $Ma=0.4$.

e) The maximum working condition the probe utilized in is total pressure 1036kPa and temperature 1760 K. The distribution of coolant film on the probe in the experiments consists appropriately with the CFD simulation result.

References:

[1] YANG Can, XIONG Yibin. High temperature thermocouple sensor: China, ZL2009 20109714.5[P]. 2010-05-19. (in Chinese)

[2] YANG Can, WU Weili, XIONG Yibin, et al. Calibration technology of high-temperature thermocouple for combustor exit of an aero-engine[J]. Journal of Aerospace Power, 2016, 31(4): 769-774. (in Chinese)

[3] LIU Liping, XUE Xiusheng, SUN Qi, et al. Development and application of high-accuracy water cooled high temperature thermocouple[J]. Aeroengine, 2009, 35(4): 48-50. (in Chinese)

[4] PLANA V, VAUTHIER J S, CASTELOOT C. Design and optimization of a high temperature water cooled probe for gas analysis measurement on K11 combustion test rig[R]. ASME Paper GT2011-45177, 2011.

[5] WANG Mingrui, WANG Zhenhua, HAN Bing, et al. High temperature measurement technology for main combustion chamber of aeroengine[J]. Aeroengine, 2016, 42(5): 87-93. (in Chinese)

[6] ANDERSON J D. Fundamentals of aerodynamics[M]. 5th ed. Berkshire: McGraw-Hill, 2011.

[7] HAN J C, DUTTA S, EKKAD S. Gas turbine heat transfer and cooling technology[M]. Abingdon: Taylor & Francis Books, Inc, 2001.

[8] GOLDSTEIN R J, ECKERT E R G, BURGGRAF F. Effects of hole geometry and density on 3-dimensional film cooling[J]. International Journal of Heat and Mass Transfer, 1974, 17(5): 595-607.

[9] HAVEN B A, KUROSAKA M. The effect of hole geometry on lift-off behavior of coolant jets[R]. AIAA 96-0618, 1996.

[10] EKKAD S V, HAN J C. A review of hole geometry and coolant density effect on film cooling[R]. ASME Paper HT2013-17250, 2013.

[11] HAN J C, TENG S. Effect of film-hole shape on turbine blade film cooling performance[J]. Journal of Thermophysics & Heat Transfer, 2012, 15(3): 257-265.

[12] HYAMS D G, LEYLEK J H. A detailed analysis of film cooling physics: Part Ⅲ streamwise injection with shaped holes[R]. ASME Paper 97-GT-271, 1997.

[13] CHEN A F, LI S J, HAN J C. Film cooling with forward and backward injection for cylindrical and fan-shaped holes using PSP measurement technique[R]. ASME Paper GT2014-26232, 2014.

[14] LIU K, YANG S F, HAN J C. Influence of coolant density on turbine blade film-cooling with axial shaped holes[J]. Journal of Heat Transfer, 2014, 136(4): 044501.1-044501.5.

[15] DIGANTA P N, LIU K C, AKHILESH P R, et al. Influence of coolant density on turbine blade film-cooling using pressure sensitive paint technique[J]. Journal of Turbomachinery, 2012, 134(3): 1529-1540.

[16] Northwestern Polytechnical University. Measurement of aerodynamic parameters in aero engine[M]. Beijing: National Defend Industry Press, 1980: 31-34. (in Chinese)

[17] Beijing Aero Material Research Institute. Material handbook for aero engine design[M]. Beijing: Aviation Industry Corporation of China, 1989.

[18] CAO Yuzhang. Heat transfer in aero engine[M]. Beijing: Beijing University of Aeronautics and Astronautics Press, 2005: 92-97. (in Chinese)

[19] HOLMAN J P, ROHSENOW W M. Heat transfer[M]. 10th ed. Berkshire: McGraw-Hill, 2010.

(编辑:李岩梅)